euspen's 18th International Conference & Exhibition, Venice, IT, 2018
www.euspen.eu

Feasibility study of hybrid spindle system with ball and electromagnetic bearings for suppression of chatter vibrations during milling with a small end mill

Eiji KONDO[1], Mitsunari ODA[2] and Daisuke TABUCHI[1]

[1]*Kagoshima University*
[2]*Makino Milling Machine Co. Ltd.*

kondo@mech.kagoshima-u.ac.jp

Abstract
In the end milling process, it is very important to prevent the occurrence of chatter vibrations because they can cause problems such as the reduction of tool life, tool fracture, and deterioration of the machined surface quality. The aim of this study was to theoretically investigate a hybrid spindle system with a ball bearing at one end and an electromagnetic bearing at the other for the suppression of chatter. The equation of state for the proposed spindle control system was derived under the assumptions that the silicon steel cylinder was subjected to an electromagnetic controlling force and the end mill was subjected an external force at its lower end. It was demonstrated that the stability limit for regenerative chatter with state feedback was approximately three times that without state feedback when the feedback coefficient was determined by the pole assignment of the control system under the assumption that the real part of the roots calculated from the characteristic equation for the system increased by three times.

Electromagnetic Force, Hybrid Spindle System, State Feedback Control, Suppression, End Milling, Chatter Vibrations

1. Introduction

In the end milling process, it is very important to prevent the occurrence of chatter vibrations because they can cause problems such as the reduction of tool life, tool fracture, and deterioration of the machined surface quality. Consequently, numerous studies on the suppression of chatter vibrations have been carried out [1] [2]. Spindles with electromagnetic bearings may enable the suppression of chatter with suitable magnetic force control; however, it is difficult to control electromagnetic bearing systems, and the allowance of the cutting force is very small [3] [4]. This study theoretically considers a hybrid spindle system with a ball bearing at one end and an electromagnetic bearing at the other for the suppression of chatter during end milling. The proposed system is more easily controlled, and could allow a larger cutting force than a spindle system supported by only electromagnetic bearings.

2. Hybrid spindle system

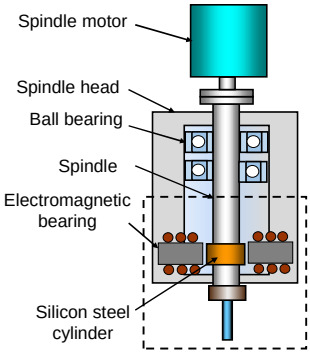

Figure 1. Schematic of proposed hybrid spindle system with ball and electromagnetic bearings

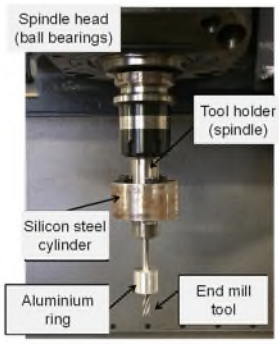

Figure 2. Tool holder with end mill as dummy spindle system in spindle head

Figure 1 shows a schematic of the proposed hybrid spindle system for use with an end mill. At the upper end, the spindle is supported only by ball bearings without any electromagnetic bearings. Consequently, the end mill can be deflected by the force generated by the electromagnetic bearing. Figure 2 shows the dummy spindle system with a silicon steel cylinder subjected to an electromagnetic force and an end mill in a spindle head, corresponding to the area indicated by the dashed line in Fig. 1.

3. Dynamic model of spindle with end mill

Table 1 lists the modal parameters for the silicon steel cylinder and the lower end of the end mill shown in Fig. 2 obtained by impact testing. In the impact test of the silicon steel cylinder, a micro-accelerometer was attached to the cylinder, and the cylinder was impacted by a hammer. In the impact test of the end mill, the micro-accelerometer was attached to the lower end of the end mill. Table 2 lists the free vibration characteristics calculated from the modal parameters given in Table 1. Figure 3 shows a dynamic model of the spindle with the end mill. The equations of motion for the hybrid spindle with the end mill are

Table 1 Modal parameters for the tool holder with the end mill

Silicon steel cylinder	Natural frequency	590 Hz
	Damping ratio	15 %
End-mill at bottom end	Natural frequency	625 Hz
	Damping ratio	0.7 %

Table 2 Free vibration characteristics of the tool holder with the end mill

Silicon steel cylinder	Mass	1.4 kg
	Spring constant	19.24×10^6 N/m
	Damping coefficient	155.7 N・s/m
End-mill at bottom end	Mass	0.01 kg
	Spring constant	0.15×10^6 N/m
	Damping coefficient	155.7 N・s/m

$$m_1\ddot{x}_1 = f_a - k_1x_1 + k_2(x_2 - x_1) - c_1\dot{x}_1 + c_2(\dot{x}_2 - \dot{x}_1)$$
$$m_2\ddot{x}_2 = f_2 - k_2(x_2 - x_1) - c_2(\dot{x}_2 - \dot{x}_1) \quad (1)$$

where m_1 is the mass of the silicon steel cylinder, m_2 is the mass of the end mill concentrated at the lower end, x_1 and x_2 are the respective displacements of m_1 and m_2, k_1 and k_2 are their respective spring constants, c_1 and c_2 are their respective damping coefficients, f_2 is the external force applied to the lower end of the end mill, and f_a is the electromagnetic force shown in Fig. 3. The equation of state for the spindle with the end mill can be derived from Eq. (1) as

$$\frac{d\mathbf{z}(t)}{dt} = \mathbf{A}\mathbf{z}(t) + \mathbf{B}_1u(t) + \mathbf{B}_2w(t), \quad u(t) = f_a, \quad w(t) = f_2 \quad (2)$$

$$\mathbf{z}(t) = \begin{bmatrix} z_1 \\ z_2 \\ z_3 \\ z_4 \end{bmatrix} = \begin{bmatrix} x_1 \\ \dot{x}_1 \\ x_2 \\ \dot{x}_2 \end{bmatrix} \quad \mathbf{B}_1 = \begin{bmatrix} 0 \\ 1/m_1 \\ 0 \\ 0 \end{bmatrix} \quad \mathbf{B}_2 = \begin{bmatrix} 0 \\ 0 \\ 0 \\ 1/m_2 \end{bmatrix}$$

$$\mathbf{A} = \begin{bmatrix} 0 & 1 & 0 & 0 \\ -\left(\frac{k_1}{m_1} + \frac{k_2}{m_1}\right) & -\left(\frac{c_1}{m_1} + \frac{c_2}{m_1}\right) & \frac{k_2}{m_1} & \frac{c_2}{m_1} \\ 0 & 0 & 0 & 1 \\ \frac{k_2}{m_2} & \frac{c_2}{m_2} & -\frac{k_2}{m_2} & -\frac{c_2}{m_2} \end{bmatrix}.$$

The characteristic roots s_i of Eq. (2) can be calculated from $|s\mathbf{I} - \mathbf{A}| = 0$, where s is the Laplace operator and $\mathbf{I}$ is the identity matrix, as

$$s_1 = -36.32 + 4019j, \quad s_2 = -36.32 - 4019j$$
$$s_3 = -46.98 + 3622j, \quad s_4 = -46.98 - 3622j.$$

When the state feedback expressed by Eq. (3) is applied to the spindle system, the equation of state can be expressed by Eq. (4).

$$u(t) = -\mathbf{K}\mathbf{z}(t), \quad \mathbf{K} = \begin{bmatrix} K_1 & K_2 & K_3 & K_4 \end{bmatrix}^T \quad (3)$$

$$\frac{d\mathbf{z}(t)}{dt} = \mathbf{P}\mathbf{z}(t) + \mathbf{B}_2w(t), \qquad \mathbf{P} = \mathbf{A} - \mathbf{B}_1\mathbf{K} \quad (4)$$

$$x_2(t) = \mathbf{C}\mathbf{z}(t), \quad \mathbf{C} = \begin{bmatrix} 0\,1\,0\,0 \end{bmatrix}^T. \quad (5)$$

The frequency response function with an external force f_2 as the input and the displacement of the end mill x_2 as the output is derived by taking the Fourier transform of Eqs. (4) and (5). The response function $G(j\omega)$, which is defined as the ratio of the Fourier transforms $X_2(j\omega)$ and $F_2(j\omega)$ of x_2 and f_2, where ω is the angular frequency, is expressed as

$$G(j\omega) = \frac{X_2(j\omega)}{F_2(j\omega)}, \quad \frac{X_2(j\omega)}{F_2(j\omega)} = \mathbf{C}(j\omega\mathbf{I} - \mathbf{P})^{-1}\mathbf{B}_2. \quad (6)$$

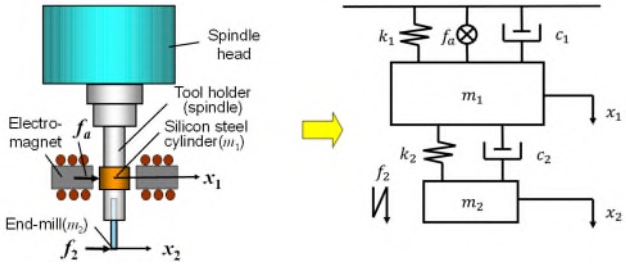

Figure 3. Dynamic model of spindle with end mill

4. Pole assignment of control system

The characteristic roots λ_i of Eq. (4) can be calculated from $|s\mathbf{I} - (\mathbf{A}-\mathbf{B}_1\mathbf{K})| = 0$. Consequently, if the real parts of the characteristic roots λ_1 and λ_2 are assumed to be three times the real parts of the characteristic roots s_1 and s_2 for the end mill vibration, the state feedback coefficient K can be expressed as

$$\lambda_1 = -109.0 + 4019j, \quad \lambda_2 = -109.0 - 4019j$$
$$\lambda_3 = -46.98 + 3622j, \quad \lambda_4 = -46.98 - 3622j$$
$$\mathbf{K} = \begin{bmatrix} K & K_2 & K_3 & K_{41} \end{bmatrix}^T = \begin{bmatrix} 24363 & 203.36 & -11798 & -30.32 \end{bmatrix}^T.$$

5. Dynamic characteristics of end mill with magnetic control

Figure 4 shows the compliance at the lower end of the end mill with state feedback calculated from Eq. (6). The compliance without state feedback, $|G_c|$, is represented by the black curve. The compliance with state feedback, $|G_a|$, is represented by the red curve and is one third of that with state feedback at the peak around 640 Hz. When only the state of the lower end of the end mill was used for feedback control, the compliance in this case, $|G_b|$ (blue curve), was about 20% less than that ($|G_c|$) without state feedback at the peak around 640 Hz. Figure 6 shows the real part of the frequency response function given in Eq. (6), $\mathrm{Re}[G]$. The stability limit of regenerative chatter is inversely proportional to the local minimum of the real part of the frequency response function, $\mathrm{Re}[G]_{\min}$. Consequently, Fig. 5 indicates that the stability limit for regenerative chatter with state feedback, which is proportional to $1/\mathrm{Re}[G_a]$, at a frequency of approximately 640 Hz, is approximately three times that without state feedback, which is proportional to $1/\mathrm{Re}[G_c]$.

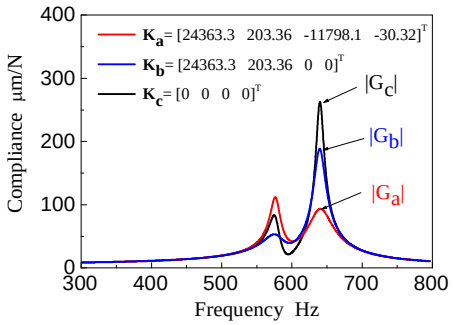

Figure 4. Compliance of lower end of end mill with state feedback

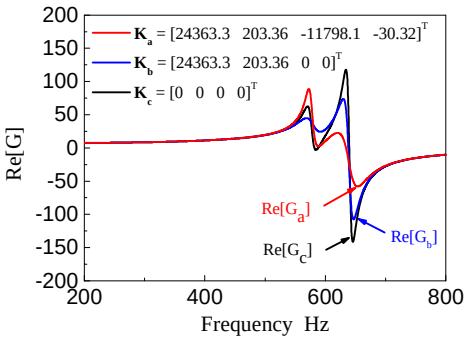

Figure 5. Real part of frequency transfer function with state feedback

6. Conclusions

In this study, it was theoretically demonstrated that the stability limit for regenerative chatter with state feedback could be increased approximately threefold relative to that without state feedback when the feedback coefficient was determined based on the pole assignment of the control system under the assumption that the real parts of the roots calculated from the characteristic equation for the system increased by three times.

References

[1] Quintana G and Ciurana J 2011 Int. J. Machine Tools & Manufact. **51** 363-376

[2] Fukagawa S, Fujimoto H, Terada Y and Ishii S 2015 IECON 2015 – 41st Annual Conference of the IEEE Industrial Electronics Society DOI: 10.1109/IECON.2015.7392525

[3] Gourc E, Seguy S and Arnaud L 2011 Int. J. Machine Tools & Manufact. **51** 928-936

[4] Huang T, Chen Z, Zhang H T and Ding H 2015 J. Dyn. Sys., Meas., Control **137** 111003